JTTEE5 17:637–645
DOI: 10.1007/s11666-008-9237-6
1059-9630/$19.00 © ASM International

Effects of Surface Chemistry on Splat Formation During Plasma Spraying

A.T.T. Tran, M.M. Hyland, T. Qiu, B. Withy, and B.J. James

(Submitted May 2, 2008; in revised form September 21, 2008)

Ni-Cr single splats were plasma-sprayed at room temperature onto aluminum and stainless steel substrates, which were modified by thermal and hydrothermal treatments to control the oxide surface chemistry. The proportions of the different splat types were found to vary as a function of substrate pretreatment, especially when the pretreatment involved heating. It was observed that surface roughness did not correlate with changes in splat morphology. Substrate surfaces were characterized by X-ray photoelectron spectroscopy using in situ heating in vacuum to determine the effect of thermal pretreatment on substrate surface chemistry. It was found that the surface layers were composed primarily of oxyhydroxides. When the substrates were heated to 350 °C, water vapor was released from the dehydration of oxyhydroxide. Preheating the substrate can remove the water prior to spraying: preheated substrates had improved the physical contact between the splat and substrate, which enhanced the formation of disk splats and increased the number of splats.

Keywords plasma spray, preheating substrate, roughness effect, surface chemistry

1. Introduction

The nature of the interface between splat and substrate in thermal spray coating is important in determining the mechanical, thermal, and electrical properties of the coatings. Bonding formation and splat morphology are profoundly influenced by the substrate temperature and the substrate surface oxide layer (Ref 1-11). Fukumoto (Ref 1-5) and others (Ref 8, 10, 11) have shown that splat morphology changes from an unfavorable splash splat shape to a favorable disk splat shape when the substrate is heated over a narrow range of temperatures. The underlying cause of the change in splat morphology is not clearly understood. It has been attributed to desorption of gases (Ref 7, 8, 11, 12), oxidation of the surface (Ref 3, 9), and changes in surface roughness (Ref 1, 3). Jiang (Ref 11) showed that the contact area between splat and substrate is increased and the adhesion is improved on substrates where the adsorbed gas has been removed or reduced. However, heating can also result in changes in the thickness and roughness of the surface layer, which may also affect the splat formation process. Fukumoto et al. (Ref 1) suggested that the thickness of the oxide layer and increased surface roughness on the nanoscale level result in a better wetting ability at the interface of substrate and splat when substrates were heated or preheated, consequently promoting disk splat formation. In the same study, no changes in chemical composition could be detected, supporting the greater importance of surface roughness rather than surface chemistry on splat morphology. Later studies (Ref 3, 4), however, suggested that the nanoscale roughness was not a dominant factor, since gold-coated preheated substrates, having increased surface roughness on the nanoscale, did not result in disk splat morphology. There were also no significant changes in splat morphology of Mo particles on nonheated and heated glass substrates (Ref 10). McDonald et al. (Ref 12) have recently shown that the average roughness on a nanometer scale had lesser influence on the splat morphology than attached adsorbates. Thus, surface roughness does not appear to be a critical character in splat morphology.

All metals are covered with oxide layers of variable composition and thickness, depending strongly on the local environment, pretreatments, and a variety of other parameters. The surface layers on aluminum and stainless steel formed under ambient conditions are mixtures of oxides and oxyhydroxides (Ref 13-18). Heat treatment causes changes in the relative amounts of these species and consequent release of gases from the surface (Ref 19-23) and can also induce segregation of elements to the surface due to differences in free energy of formation oxides (Ref 24, 25). Such changes can only be detected by high resolution surface spectroscopic analysis. A recent study of single splats of HVAF-sprayed PEEK on aluminum substrate has shown that surface chemistry can

This article is an invited paper selected from presentations at the 2008 International Thermal Spray Conference and has been expanded from the original presentation. It is simultaneously published in *Thermal Spray Crossing Borders, Proceedings of the 2008 International Thermal Spray Conference*, Maastricht, The Netherlands, June 2-4, 2008, Basil R. Marple, Margaret M. Hyland, Yuk-Chiu Lau, Chang-Jiu Li, Rogerio S. Lima, and Ghislain Montavon, Ed., ASM International, Materials Park, OH, 2008.

A.T.T. Tran, M.M. Hyland, T. Qiu, B. Withy, and **B.J. James**, Chemical & Materials Engineering Department, The University of Auckland, Private Bag 92019 Auckland, New Zealand. Contact e-mail: atra021@aucklanduni.ac.nz.

affect the polymer splat formation process (Ref 26). Hence, the aim of this work was to understand the role of both surface chemistry and surface roughness on splat formation and splat morphology. The methodology was to control the surface chemistry and roughness of aluminum and stainless steel substrates by subjecting them to particular surface treatments, to characterize the resultant surface chemistries using high resolution X-ray photoelectron spectroscopy, and to look at the correlation of surface chemistry and surface morphology with the resultant NiCr splat morphologies.

2. Experimental Details

In this work, aluminum 5052 (Al) and stainless steel 304 (SS) substrates were mechanically polished to a mirror-like surface finish. Four different pretreatments were used to control the chemistry of the surface oxide: polished (P), polished and thermally treated (PT), boiled (B), and boiled and thermally treated (BT). The hydrothermally treated samples (B, BT) were boiled in deionized water for 30 min. The subsequent thermal treatment of boiled or polished samples was carried out in air at 350 °C for 90 min. All samples were stored in a dessicator to preserve the surface chemistry until they were ready to be sprayed. The time between removing from the dessicator and spraying ranged from 10 to 60 min. One set of the substrate samples was used to evaluate the effect of surface roughness on the splat shape by atomic force microscope (AFM, NanoScope IIIa) using a scan size of 100 μm. The other set of 8 samples was sprayed with molten Ni80-Cr20 alloy particles (Sulzer Metco 43VF-NS, Switzerland, $-45+5$ μm) at room temperature using a plasma spray technique. All substrates were sprayed at the same time, to allow for direct comparison of the splat morphologies, since all samples would have been exposed to the same particle size distributions and splat temperature. Plasma spraying was carried out with a Sulzer Metco 7MB gun operating at a current of 550 A and a voltage of 74 V. The spray distance was 80 mm. The powder was injected at a feeding rate of 1 g/min. The plasma gas mixture was nitrogen and hydrogen, at a flow rate of 47.6 SLPM and 5.4 SLPM, respectively. Collected splats on ($25 \times 50 \times 3$ mm) substrates were characterized qualitatively and quantitatively by Scanning Electron Microscopy (SEM) and ImageJ imaging software (National Institute of Health, Washington DC). The SEM is a Philips FEGXL30.

To examine the effect of temperature on the substrate surface chemistry, in particular the release of water or adsorbates, the polished and hydrothermal-treated samples were analyzed with X-ray Photoelectron Spectroscopy (XPS), using a Krastos Ultra Axis DLD. The samples were heated in situ in the XPS to determine the variation of surface composition with temperature. Wide scans (0-1000 eV) and narrow scans of Al 2p, Fe 2p, O 1s and C 1s at different temperatures were collected; the measured binding energies were referenced to C1s at 285.0 eV. The narrow scans were fitted by CasaXPS software with a mixture of Gaussian (G) and Lorentzian (L) for the peak shape. The fitting method was based on the established literature for aluminum (Ref 19, 20, 22) and stainless steel (Ref 21, 23).

3. Results and Discussion

3.1 Splat Characterization

Collected splats were examined using SEM to assess the effect of substrate pretreatment on the morphology of the splat. Backscattered images were used to distinguish between splat and substrate. Approximately 40 backscattered electron images at low magnification (100× to 200×) and secondary electron images at high magnification were acquired at random locations for every sample. From these images, a minimum of five random areas with around 300 splats were analyzed using ImageJ to obtain quantitative and qualitative information on splat morphologies. The obtained information included feret diameter, area, circularity, and perimeter of the individual splats. The feret diameter is the longest distance between any two points on the boundary of the splat. Typical images of collected NiCr splats on aluminum and stainless steel substrates are shown in Fig. 1. A splat classification

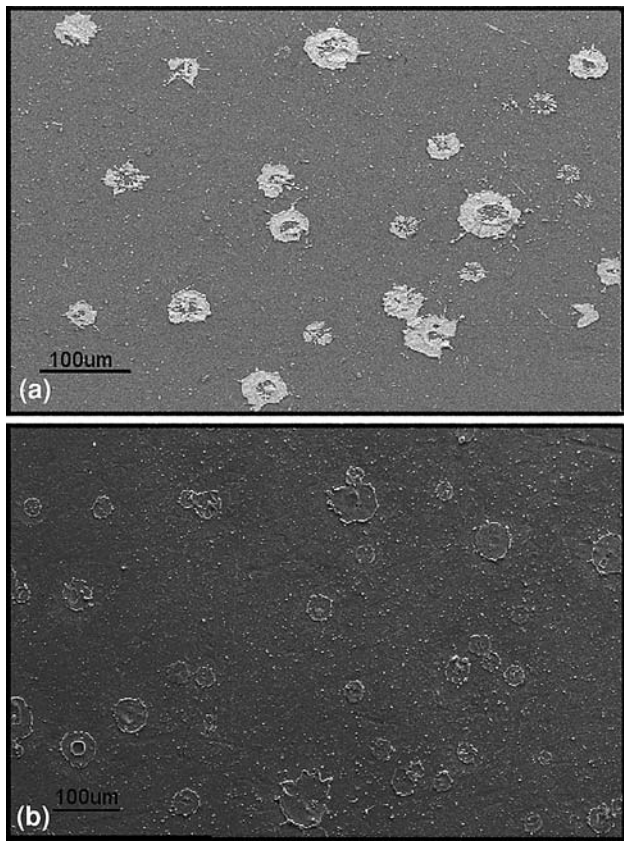

Fig. 1 Typical images of collected NiCr splats on (a) aluminum and (b) stainless steel substrates

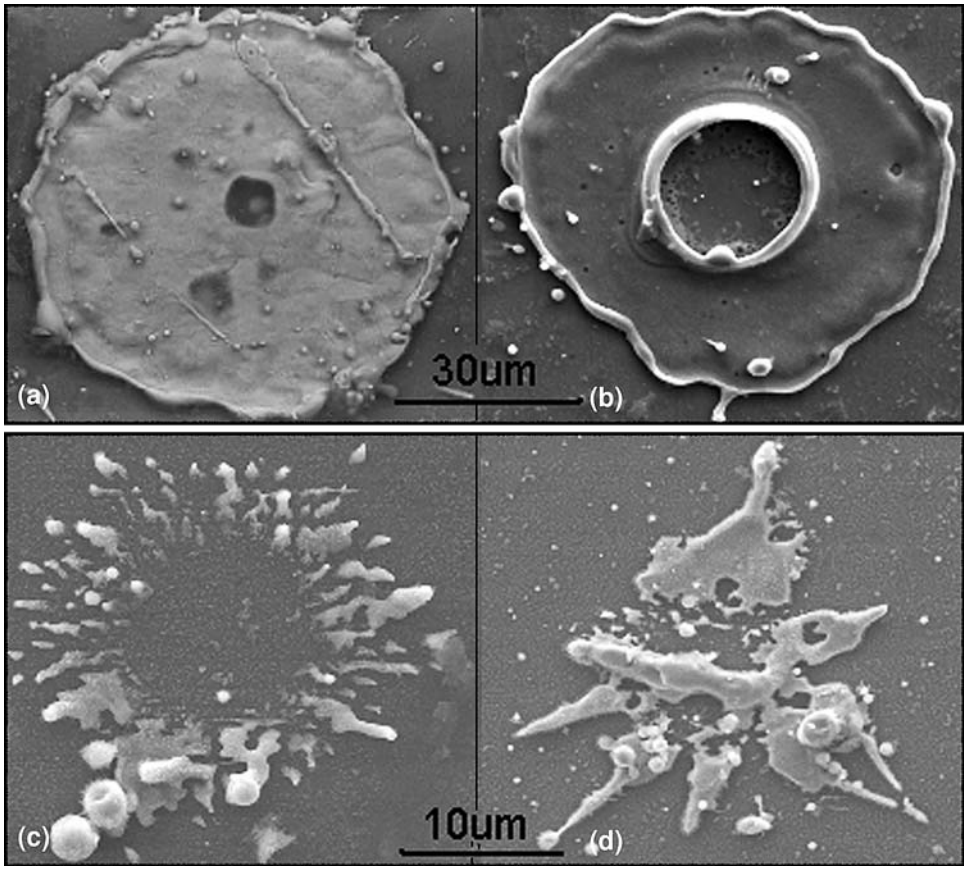

Fig. 2 Two subcategories of disk splat: (a) round disk splat and (b) doughnut disk splat; and of splash splat, (c) round splash splat and (d) irregular splash splat

scheme was developed based on two primary morphologies: splash and disk-type splats. In addition, these splat types were divided into two subcategories: (a) round and (b) doughnut disk splats, and (c) round and (d) irregular splash splats as shown in Fig. 2. The proportion of each of these splat types was quantified for all sprayed samples.

Collected disk splats had a reasonably round shape, a flat surface, and some small fingers indicating the deposition of completely molten NiCr droplets. Round disk splats are here defined as splats whose center pore diameter was smaller than 4 μm. Doughnut disk splats are defined as round disk splats with a center bubble-like hole having a diameter larger than 4 μm. Micropores of approximately 1 μm and curling up at the edges of splats were also observed. It was also observed that there was no splat formation on boiled aluminum substrates. Instead, impact marks were observed on the surface as in Fig. 3.

The results of image analysis using ImageJ tool are shown in Fig. 4. Because there was no splat formation on boiled aluminum substrates, no data were available for these samples. It was found that the splat distribution and splat morphology on aluminum and stainless steel had a similar trend with pretreatment. For both substrate types, the splat density, diameter, and percentage of splats as disk splats increased markedly on preheated substrates compared to non-preheated substrates. For example, as shown in Fig. 4, the splat density on the polished aluminum substrates increased by 40% as a result of preheating. Disk splats were found on both non-preheated and preheated aluminum substrates, but in very different proportions (Fig. 4b). It was observed that there were no round disk splats and only approximately 5% doughnut disk splats (with the average diameter of 42.5 μm) formed on Al_P surface. However, the disk splat proportion was sharply increased for preheated substrate with 17% of round disk splat and 26% of doughnut disk splat. In addition, the average diameter of disk splats increased by about 12% for preheated substrates compared to non-preheated substrates.

A general linear trend showing increasing splat density and disk splat proportion with preheating substrate was also observed on stainless steel substrate. The image analysis results show that for the stainless steel substrates, the boiled substrate surface clearly had the least splats adhering to it. The SS_P and SS_BT surfaces had a similar number of splats whereas SS_PT surface had the most splats. The increase of splat density on the preheated stainless steel substrates was 14% (PT) and 4% (BT) relative to their non-preheated counterparts. In addition, the number of micropores noticeably decreased upon heat treatment. More micropores were found on boiled stainless steel substrates than on polished surface; however, the

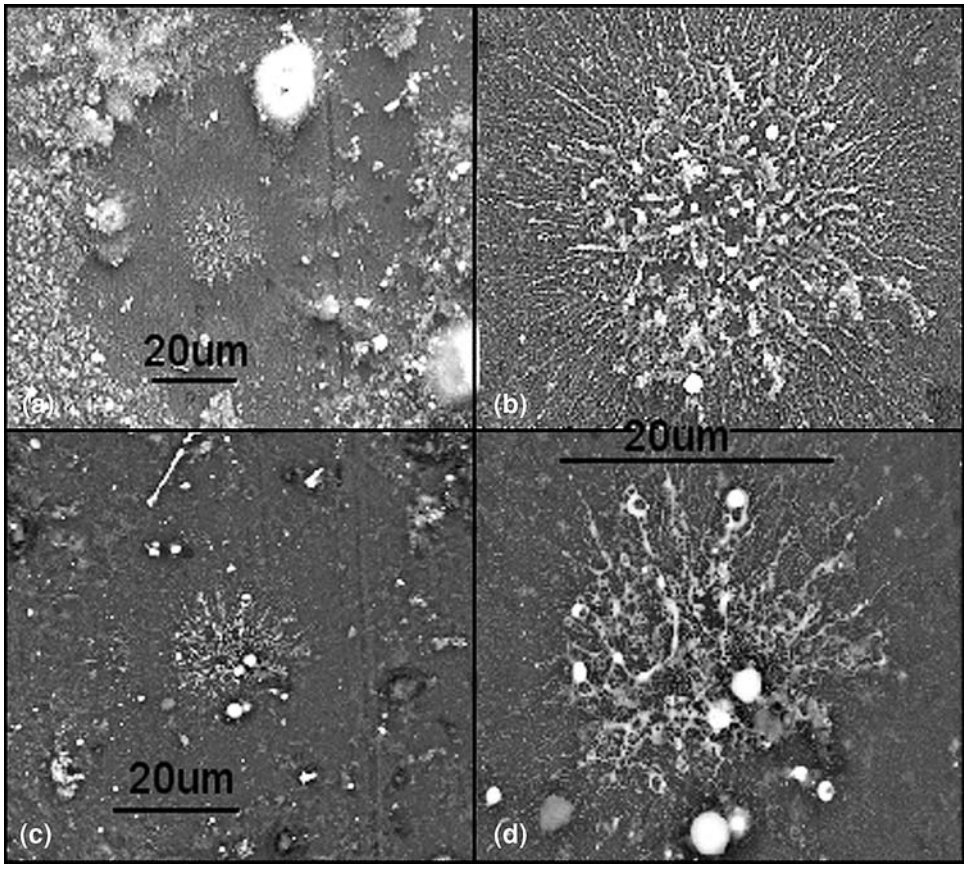

Fig. 3 Impact marks by NiCr droplets on (a) Al_B, (b) enlargement of (a), (c) Al_BT, and (d) enlargement of (c)

number of micropores was similar after heat treatment. Unexpectedly, micropores were mainly found in splats deposited on stainless steel substrate compared to aluminum substrates.

On non-preheated stainless steel substrates, the SS_P surface clearly had a smaller proportion of disk splats (45%), with a similar diameter to those on Al_P, while SS_B had higher proportion disk splats of (63%) with an average diameter of 50.2 μm. More important, preheating the substrates resulted in a significant decrease in the amount of irregular splash splats and an increase in the number of round disk splats. It was expected that some doughnut disk splats converted to round disk splats on preheated substrates. The average diameter of disk splats on stainless steel also increased by 12 to 14% for preheated substrates compared to non-preheated substrates.

It was also found that splat density and proportion of disk-type splats were significantly higher on stainless steel than on aluminum substrates, indicating that the adhesion of NiCr splats on stainless steel was much better than on aluminum. Unlike boiled aluminum substrates, there was splat formation on boiled stainless steel. It was expected that the wetting ability of impacting NiCr splats on boiled sample would decrease compared to that on polished sample. However, experiments showed the reverse trend with disk splat fraction of 45% on polished sample and 63% on the boiled one. When these substrates were preheated, they had similar proportions of disk splats.

3.2 Surface Roughness

Surface roughness was evaluated by two parameters: the average surface roughness (Ra) and skewness (Sk). Ra gives the average distance between the surface and mean centerline, but does not discriminate very well between peaks and valleys. Skewness is used to measure the height distribution. A negative skewness value indicates that the sample has more valleys than peaks, and the reverse for a positive skewness value (Ref 27).

The roughness results of aluminum substrate with different pretreatment types, evaluated by AFM on a scan size of 100 μm, are tabulated in Table 1. It was observed that there were no significant differences in both Ra and Sk for polished aluminum and polished and thermally treated aluminum. In these cases, the small negative value of Sk was obtained because peaks are more easily polished than valleys (Ref 27).

In contrast, surface roughness changed slightly on the hydrothermally treated samples. Boiling the aluminum substrate in deionized water for 30 min induced a change to a surface topography consisting of more valleys with slightly higher value of Ra compared to that of polished

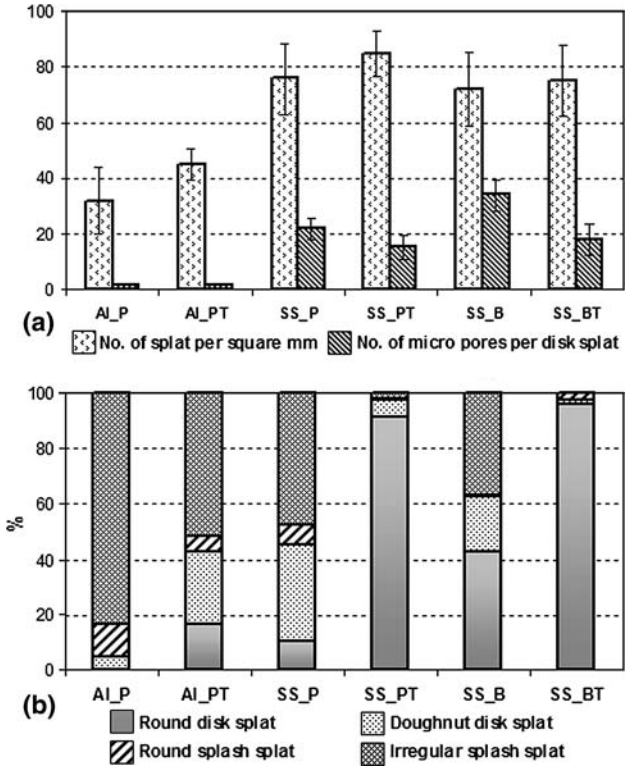

Fig. 4 Effect of surface pretreatment on the (a) splat density and number of micropores per disk-type splat with a standard deviation of 90% confidence and (b) splat distribution

Table 1 Surface roughness results

Substrates	Ra, nm	Sk
Al_P	11.6	−0.14
Al-PT	14.7	−0.14
Al-B	39.8	−0.41
Al-BT	15.1	0.22

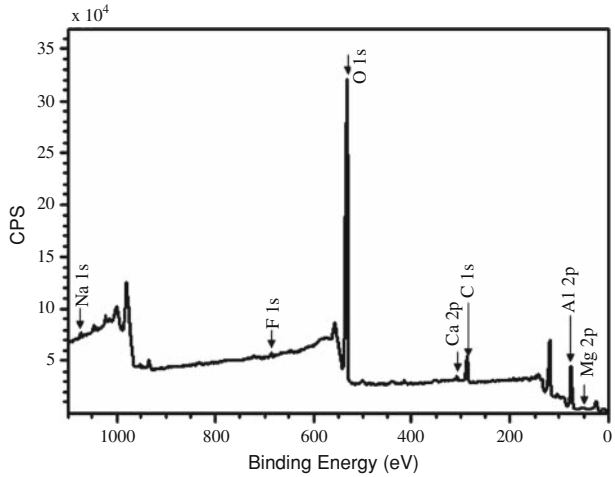

Fig. 5 Wide scan of Aluminum sample

samples. Preheating the boiled aluminum produced a smoother surface with a positive Sk value and an Ra value similar to that of polished samples.

Although there was no significant difference in the measured surface roughness between non-preheated and preheated polished aluminum substrates, the splat density and disk splat fraction greatly improved with preheat treatment. In addition, there was no splat formation on boiled aluminum substrates regardless of different surface roughness values. These results suggest that the differences in splat morphology between preheated and non-preheated substrates are not due to a surface roughness effect.

3.3 XPS Results

The change in surface chemistry due to preheating of aluminum and stainless steel was studied using XPS over a range of temperatures from ambient to 350 °C. A typical wide scan of polished aluminum sample at ambient temperature is shown in Fig. 5. The sample contained minor levels of impurities—Na, Ca, and F—due to contamination from tap water during washing and polishing.

The Al 2p envelopes were fitted by three different photopeaks. They are metal peak (~73.2-73.3 eV), oxide peak (~76.1-76.3 eV), and oxyhydroxide peak (~78.3-78.6 eV) (Fig. 6a) (Ref 20, 28). The surface oxide thickness (d, nm) was estimated from the Al 2p peak oxide/metal peak ratio using literature value for escape depth for the Al 2p photopeak (Ref 19).

The calculated oxide thickness of polished aluminum sample at room temperature and 350 °C was 5 and 6.4 nm, respectively. In contrast, the absence of metal peak in the Al 2p core level of boiled samples at ambient condition and 350 °C (Fig. 6b) indicated that the films formed by these processes were thicker than XPS analysis depth (8 nm). It was estimated from Ion Beam Analysis (IBA) that the oxide layer is approximately 220 nm thick.

The O 1s peak was resolved into three different photopeaks representing the oxide (~532.6-532.9 eV), oxyhydroxide (~533.9-534.5 eV), and chemisorbed water (~535.4 V) from lowest to highest binding energy, respectively (Ref 20, 28). The narrow scans of O 1s of polished and boiled aluminum samples at specified temperatures are illustrated in Fig. 7(a) and (b), respectively. It was observed that oxyhydroxide was present on all aluminum surfaces. In the polished sample, the surface sample consisted of a layer of chemisorbed water and oxyhydroxide. The presence of these peaks was attributed to the hydration reaction of the surface with moisture, which occurs rapidly under ambient conditions (Ref 13-16). However, the oxyhydroxide proportion was much smaller than the oxide proportion. In contrast, their proportion was equal in boiled sample, as expected, since the form of oxyhydroxide here, AlOOH, should have these two species in equal stoichiometries. In addition, the

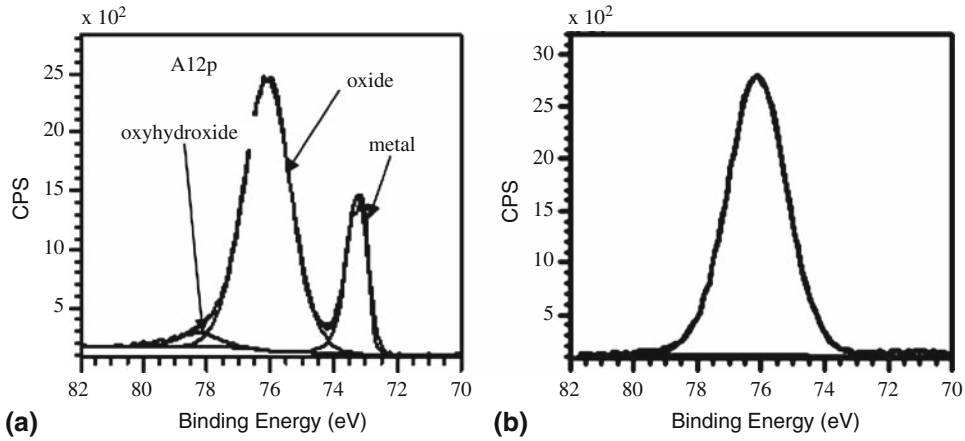

Fig. 6 Narrow scan of Al 2p (a) polished and (b) boiled/boiled and thermally treated sample

atomic ratio of O: Al in boiled sample was 2, which confirmed the formation of a surface layer of pseudo-boehmite, AlOOH (Ref 19, 20).

There was a significant change in the surface chemistry with heating, as evidenced by changes in the O 1s peak. When the temperature was raised to 100 °C with holding time of 30 min, the chemisorbed water was completely driven off. As the temperature was raised further, the oxyhydroxide gradually decreased in intensity and the oxide increased, on both polished and boiled aluminum. This is evidence that the oxyhydroxide is dehydrating, releasing water vapor as a product, and converting to oxide. This process, which also takes place in bulk aluminum oxides, begins at about 275 °C and is completed by 350 °C (Ref 16). For the thin surface oxyhydroxide/oxide layers on polished substrates, the entire surface layer was completely dehydrated in the 30-min treatment time. However, this cannot be confirmed for the much thicker layers on boiled substrates. Certainly the outermost 5-6 nm were dehydrated, but because the XPS can only probe the top 8 nm of the surface, the degree of dehydration of the underlying layers could not be established. The pretreatment also caused the surface oxide to increase slightly in thickness, from 5 to 6.4 nm. XPS was also carried out on stainless steel substrate. The results, not shown here, confirmed that, like the aluminum substrates, the surface of the stainless steel was composed of a thin layer of oxyhydroxide.

Some surface enrichment of minor elements, Mg in the case of aluminum and Cr in the case of stainless steel, was observed as a result of preheating (Table 2). However, there was no Mg segregation on pretreated boiled aluminum samples.

In short, the considerable change in surface chemistry at 350 °C suggests that under spraying conditions, when the hot droplet impacts the sample, the oxyhydroxide will dehydrate, releasing water as a gas that can affect the splat spreading process. In addition, the segregation of Mg and Cr to the surface may also affect the wettability (Ref 29) of the surfaces and thus also affect the splat formation process.

4. Discussion

The surface layer of all non-preheated substrates consists of a mixture of oxide, oxyhydroxide, and chemisorbed water, in varying proportions. The existence of this layer is due to the hydration reaction of the surface oxide with atmospheric moisture. Preheating results in dehydration: i.e., the release of water, first from the chemisorbed species at about 100 °C and then again between 300 and 350 °C, due to the conversion of the oxyhydroxide to oxide. A further change in the surface chemistry due to preheating was the segregation of Mg (for aluminum substrates) and Cr (for stainless steel substrates) at the surface. At the same time, the thickness of the oxide layer on polished substrates increases, but the roughness of this layer does not change significantly. Thus, the significant improvements of splat density, disk-type splat proportion, and the average diameter of disk splat with preheating are probably the result of the chemical changes at the substrate surface (prior removal of oxyhydroxide), rather than surface roughness. It is proposed that when the molten droplet impacts the substrate at high temperature, the dehydration of oxyhydroxide layer on the substrate surface to oxide occurs, and releases water vapor, which inhibits the adhesion of impinging splat. Preheating drives off water vapor resulting in better contact between splat and substrate, and hence enhancing disk splat and reducing splashing. For the relatively thin surface oxide/oxyhydroxide layers on the polished substrates, 5 nm, a 90-min pretreating time was sufficient to completely or nearly completely dehydrate the surface layer. Thus, preheating treatment was is an important parameter contributing to the formation of splat and splat shape on aluminum and stainless steel substrates because of the chemical changes, dehydration, induced at the surface.

In addition, the observed segregation of magnesium on the surface with heating is expected to affect the wetting properties of aluminum substrate. It has been reported that magnesium disrupts the oxide layer, reducing the

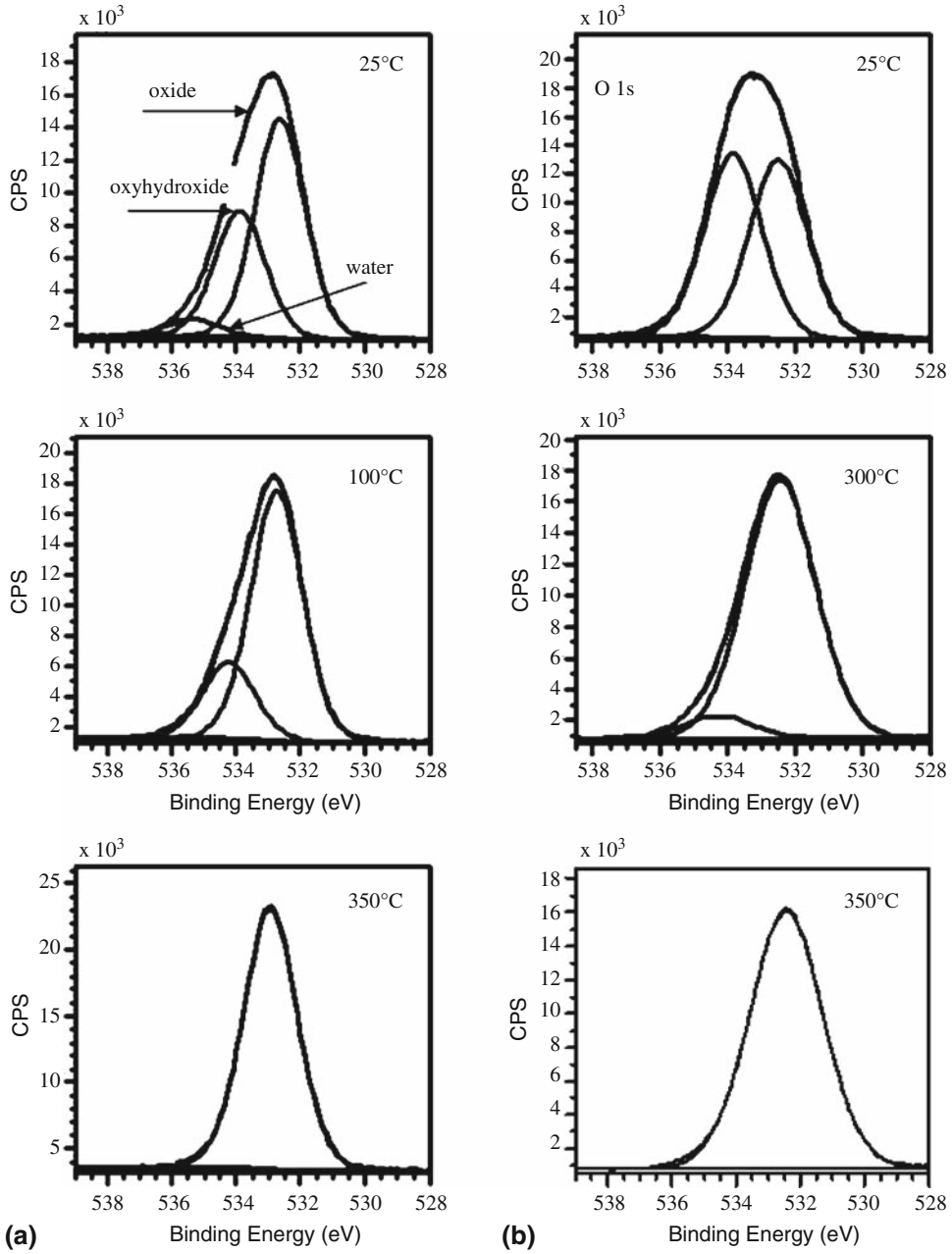

Fig. 7 Narrow scan of O1s (a) polished and (b) boiled aluminum with heating temperatures and holding time of 30 min

alumina proportion and producing clean and wettable surfaces (Ref 29). The greater the Mg proportion was on the surface, the more disk splats were formed. On stainless steel substrates, the existence of chromium on the surface improved wettability of NiCr splat on substrate thanks to its metal-like property. Thus, the difference of Cr proportion between polished and boiled stainless steel may explain the variations in disk splat fraction and also explain the difference in splat formation between boiled aluminum and boiled stainless steel substrates.

There was a complete absence of splats on boiled aluminum substrates. The boiled aluminum substrate represented the extreme example of water release from conversion of surface aluminum oxyhydroxide to oxide. These surfaces consisted of relatively thick layers (>200 nm) of an almost pure aluminum oxyhydroxide (pseudoboehmite, AlOOH). It appears that the desorption of large amount of water vapor at high temperature and thick layer of oxyhydroxide or oxide reduced the wettability of the substrate and impeded the spreading and adhesion of the splat. The reason for the lack of splat formation on the pretreated boiled aluminum is still unclear, but the greater similarity of the surface roughness with the polished substrates suggests that the answer

Table 2 Surface composition from various substrate treatments at different temperatures

Substrates	*T*, °C	O, %	Al, %	Mg, %
Al_P	20	48.2	35.2	1.2
	350	52.2	39.2	3.1
Al_B	20	60.8	30.8	0
	350	53.2	38.1	0
			Fe, %	Cr, %
St_P	20	48.9	10.9	1.4
	350	45.2	21.4	7.5
St_B	20	45.6	9.5	3.8
	350	40.3	17.5	7.2

probably lies in the surface chemistry, not surface topography. It may be that the oxyhydroxide was not completely dehydrated in the 90 min of pretreatment and subsequent water release during splat impact prevented splat formation or, alternatively, that the absence of Mg had a negative impact on the wettability.

The splat density and disk-type splat proportion were significantly higher on stainless steel substrates than on aluminum substrates, indicating that the adhesion of NiCr splats on stainless steel was much better than on aluminum. The average diameter of disk-type splat on stainless steel substrates was a little larger than that on aluminum substrates. It is speculated that the heat transfer between splat and substrate contributed to the splat density and final splat diameter. Because the thermal diffusivity of stainless steel is much smaller than that of aluminum, the solidification rate of NiCr splats on stainless steel is lower than that on aluminum. It has been found that fast solidification rate triggers the phenomena of freezing-induced splashing (Ref 30), explaining the high percentage of splash splat on aluminum substrates. In contrast, delaying solidification made the molten droplet to spread more to a round disk-type splat on stainless steel substrate before solidification occurs. As a results, the splat density, disk-type splat, and average diameter of splat were much larger on stainless steel substrates than on aluminum substrates.

5. Conclusion

The influence of preheating on splat morphologies suggests that surface chemistry, not surface roughness, is the dominating factor in the splat formation and splat shape. When the aluminum and stainless steel substrates were heated, Mg/Cr segregation and the dehydration of oxyhydroxide to oxide occurred. These changes correlated with measurable changes in splat number and morphology. The release of water due to the conversion of surface oxyhydroxide to oxide, which occurs as the hot splat impacts the surface, generates a gas layer that impedes the adhesion of the splat to the substrate. Prior conversion of the oxyhydroxide to oxide during thermal pretreatment, and thus prior removal of water, prevented this gas release, resulting in improved physical contact between the splat and substrate. In addition, the segregation of magnesium and chromium enhanced wettability of the substrate. As a result, the segregation of magnesium and chromium and/or the increase of the physical contact of splat and substrate enhanced the formation of disk splats, decreased the number of pores evident in the splats, and increased the number of splats and their diameter in preheated substrate. In addition, the complete absence of splats on boiled aluminum samples was due to the desorption of water vapor at high temperature from the thick layer of oxyhydroxide and the lack of segregation of Mg on the surface. All these factors reduced the wettability of the substrate and impeded the spreading and adhesion of the splat. However, the relative importance of each factor is not clearly identified. Therefore, more work is required to determine the separate effects of dehydration and segregation separately on the splat formation and splat shape.

Acknowledgments

The authors would like to acknowledge Tertiary Education Commission of New Zealand for Top Achiever Doctoral Scholarship. The authors thank S. Enright for surface roughness measurements.

References

1. M. Fukumoto, I. Ohgitani, M. Shiiba, and T. Yasui, Effect of Substrate Surface Change by Heating on Transition in Flattening Behavior of Thermal Sprayed Particles, *Mater. Trans.*, 2004, **45**(6), p 1869-1873
2. M. Fukumoto and Y. Huang, Flattening Mechanism in Thermal Sprayed Ni Particles Impinging on Flat Substrate Surface, *J. Thermal Spray Technol.*, 1999, **8**(3), p 427-432
3. M. Fukumoto, H. Nagai, and T. Yasui, Influence of Surface Character Change of Substrate due to Heating on Flattening Behavior of Thermal Spray Particle, *J. Thermal Spray Technol.*, 2006, **15**(4), p 759-764
4. Y. Tanaka and M. Fukumoto, Investigation of Dominating Factors on Flattening Behavior of Plasma Sprayed Ceramic Particles, *Surf. Coating Tech.*, 1999, **120-121**, p 124-130
5. M. Fukumoto, T. Yamaguchi, M. Yamada, and T. Yasui, Splash Splat to Disk Splat Transition Behavior in Plasma-Sprayed Metallic Materials, *J. Thermal Spray Technol.*, 2007, **16**(5-6), p 905-912
6. V. Pershin, M. Lufitha, S. Chandra, and J. Mostaghimi, Effect of Substrate Temperature on Adhesion Strength of Plasma-Sprayed Nickel Coatings, *J. Thermal Spray Technol.*, 2003, **12**, p 370-376
7. C. J. Li and J. L. Li, Evaporated-Gas-Induced Splashing Model for Splat Formation during Plasma Spraying, *Surf. Coating Tech.*, 2003, **184**(1), p 13-23
8. A. McDonald, M. Lamontagne, C. Moreau, and S. Chandra, Impact of Plasma-Sprayed Metal Particles on Hot and Cold Glass Surfaces, *Thin Solid Films*, 2006, **514**(4), p 212-222
9. A. A. Syed, A. Denoirjean, B. Hannoyer, P. Fauchais, P. Denoirjean, A.A. Khan, and J.C. Labbe, Influence of Substrate Surface Conditions on the Plasma Sprayed Ceramic and Metallic Particles Flattening, *Surf. Coating Tech.*, 2005, **200**(7), p 2317-2331
10. A.G. McDonald, M. Lamontagne, S. Chandra, and C. Moreau, Photographing Impact of Plasma Sprayed Particles on Metal Substrates, *J. Thermal Spray Technol*, 2006, **15**(4), p 708-716
11. X. Jiang, W. Yuepeng, H. Herbert, and S. Sanjay, Role of Condensates and Adsorbates on Substrate Surface on Fragmentation

of Impinging Molten Droplets during Thermal Spray, *Thin Solid Films*, 2001, **385**(1-2), p 132-141
12. A. McDonald, C. Moreau, and S. Chandra, Effect of Substrate Oxidation on Spreading of Plasma-Sprayed Nickel on Stainless Steel, *Surf. Coating Tech.*, 2007, **202**, p 23-33
13. W. Vedder and D. A. Vermilyea, Aluminum + Water Reaction, *Trans. Faraday Soc.*, 1969, **65**, p 561-584
14. R.S. Alwitt, The Growth of Hydrous Oxide Films on Aluminum, *J. Electrochem. Soc.*, 1974, **121**(10), p 1322-1328
15. W.J. Bernard and J.J. Randall, Jr., An Investigation of the Reaction between Aluminum and Water, *J. Electrochem. Soc.*, 1960, **107**(6), p 483-487
16. K. Wefers, and C. Misra, *Oxide and Hydroxides of Aluminium, No. 19*, Alcoa Laboratories, 1987, p 22-68
17. U.R. Evans, *The Corrosion and Oxidation of Metals. Scientific Principles and Practical Applications,* Edward Arnold, London, 1960
18. B. Withy, M. Hyland, and B. James, Pretreatment Effects on the Surface Chemistry and Morphology of Aluminium, *Int. J. Modern Phys. B*, 2006, **20**(25-27), p 3611-3616
19. M.R. Alexander, G.E. Thompson, and G. Beamson, Characterization of the Oxide/Hydroxide Surface of Aluminium Using X-ray Photoelectron Spectroscopy: A Procedure for Curve Fitting the O 1s Core Level, *Surf. Interface Anal.*, 2000, **29**(7), p 468-477
20. M.R. Alexander, G. Beamson, P. Bailey, T.C.Q. Noakes, P. Skeldon, and G.E. Thompson, The Distribution of Hydroxyl Ions at the Surface of Anodic Alumina, *Surf. Interface Anal*, 2003, **35**(8), p 649-657
21. A.P. Grosvenor, B.A. Kobe, and N.S McIntyre, Examination of the Oxidation of Iron by Oxygen using X-ray Photoelectron Spectroscopy and QUASES, *Surf. Sci.*, 2004, **565**(2-3), p 151-162
22. M.R. Alexander, G.E. Thompson, X. Zhou, G. Beamson, and N. Fairley, Quantification of Oxide Film Thickness at the Surface of Aluminium using XPS, *Surf. Interface Anal.*, 2002, **34**(1), p 485-489
23. A.P. Grosvenor, B.A. Kobe, and N.S. McIntyre, Studies of the Oxidation of Iron by Water Vapour using X-ray Photoelectron Spectroscopy and QUASES, *Surf. Sci.*, 2004, **572**(2-3), p 217-227
24. C.R. Werrett, D.R. Pyke, and A.K. Bhattacharya, XPS Study of Oxide Growth and Segregation in Aluminium-Silicon Alloys, *Surf. Interface Anal.*, 1997, **25**, p 809-816
25. N. Birks, G.H. Meier, and F.S. Pettit, *Introduction to the High-Temperature oxidations of Metals*, Cambridge University Press, 2006
26. B.P. Withy, M.M. Hyland, and B.J. James, The Effect of Surface Chemistry and Morphology on the Properties of HVAF PEEK Single Splats, *International Thermal Spray Conference: Thermal Spray Crossing Borders*, Maastricht, The Netherlands, DVS-Verlag GmbH, Düsseldorf, June 2-4, 2008, p 983-986
27. T.R. Thomas: *Rough Surfaces*, 2nd ed., Imperial College Press, 1999, Chap. 7, p 135-145
28. T. Do and N.S. McIntyre, Pressure Effects on Aluminium Oxidation Kinetics using X-ray Photoelectron Spectroscopy and Parallel Factor Analysis, *Surf. Sci.*, 1999, **440**, p 438-450
29. S. Lopez, J.R. Butruille, H.M. Dunlop, G. Tourillon, J.P. Petit, J.B. Metson, B.W. Yates, Hydration, Acido-Basicity, and Adhesion Properties of Passive Films on Aluminium: A Multitechnique Study, *Proc. Intl. Symp. Aluminum Surface Science & Technology*, Antwerp, Belgium, ATB Metallergie, May 12-15, 1997, p 143–150
30. R. Dhiman and S. Chandra, Freezing-Induced Splashing During Impact of Molten Metal Droplets with High Weber Numbers, *Int. J. Heat Mass Transfer*, 2005, **48**(25-26), p 5625-5638